Anhang A

Liste der Stationen

Code	Inst.	Breite [° N]	Länge [° O]	Höhe[m]	Seismometer
AJMR	IMD	26.4791	74.6432	540	STS-2
BLSP	IMD	22.1291	82.1318	85	STS-2
BHUJ	IMD	23.2540	69.6540	80	STS-2
BHPL	IMD	23.2410	77.4245	500	STS-2
BOKR	IMD	23.7948	85.8858	282	STS-2
BOM	IMD	18.9000	72.8167	6	STS-2
CUD	NGRI	14.4700	78.8700	400	STS-2
GOA	IMD	15.4830	73.8167	58	STS-2
HYB	G	17.4185	78.5518	510	STS-1
KARD	IMD	17.3075	74.1830	581	STS-2
MDRS	IMD	13.0680	80.2463	15	STS-2
MNGR	IMD	12.8670	74.8670	0	STS-2
PUNE	IMD	18.5295	73.8491	560	STS-2
TRVM	IMD	8.5080	76.9585	64	STS-2
VISK	IMD	17.7210	83.3287	41	STS-2

Tabelle A.1: Liste der verwendeten Breitbandstationen in Indien. Alle Stationen sind mit Seismometern vom Typ Streckeisen STS-1 bzw. STS-2 ausgestattet. IMD: India Meteorological Department, NGRI: National Geophysical Research Institute, G: GEOSCOPE

Code	Breite [° N]	Länge [° O]	Höhe[m]	Seismometer
ST09	31.4210	90.0040	4752	40T
ST11	31.5814	89.9808	4745	40T
ST12A	31.6400	89.7887	4643	L4
ST13A	31.7263	89.7030	4593	40T
ST14A	31.8001	89.6612	4528	L4
ST15A	31.8510	89.5777	4579	L4
ST16	31.8883	89.4980	4624	40T
ST16A	31.9217	89.4206	4571	L4
ST17	31.9398	89.3578	4594	40T
ST17A	31.9516	89.3099	4607	L4
ST18	31.9653	89.2693	4621	40T
ST18A	31.9746	89.2047	4621	L4
ST19A	32.1032	89.1950	4546	L4
ST21	32.2292	89.1334	4548	L4
ST21A	32.2752	89.0968	4712	L4
ST22A	32.3753	89.1003	4543	L4
ST23	32.4228	89.1077	4761	3T
ST23A	32.4714	89.0492	4743	L4
ST25	32.5371	88.9403	4881	L4
ST25A	32.6118	88.9534	4955	L4
ST26A	32.6985	88.8665	4880	L4
ST27	32.7454	88.8506	4936	L4
ST29	32.9346	88.8530	4907	3T
ST31	33.1356	88.8769	4851	3T
ST32	33.2426	88.8355	4929	40T
LUMP	31.8990	89.9320	4616	40T
STW1	32.0923	88.3064	4681	40T
NASE	31.9891	91.7056	4644	40T

Tabelle A.2: Liste der Stationen des Teilexperimentes GEDEPTH-2. Seismometer: 40T: G¨uralp 40T, 3T: G¨uralp 3T, L4: Mark L4-3D

Code	Breite [° N]	Länge [° O]	Höhe[m]	Seismometer
ST00	30.5259	90.1030	4811	STS-2
ST01	30.6498	90.1337	4794	STS-2
ST02	30.7867	90.2492	4801	STS-2
ST03	30.8475	90.1914	4796	STS-2
ST04	30.9595	90.1925	4734	STS-2
ST05	31.0400	90.1742	4833	STS-2
ST06	31.1234	90.0971	5088	STS-2
ST07	31.2280	90.0696	5080	STS-2
ST08	31.2990	90.0315	4900	STS-2
ST10	31.4927	90.0082	4669	STS-2
ST12	31.6261	89.8836	4690	STS-2
ST14	31.7705	89.7084	4599	STS-2
ST15	31.8364	89.6397	4575	STS-2
ST19	32.0589	89.1913	4602	STS-2
ST20	32.1696	89.1423	4560	STS-2
ST22	32.3327	89.1164	4809	STS-2
ST24	32.4804	88.9844	4914	STS-2
ST26	32.6611	88.9157	4816	STS-2
ST28	32.8217	88.8483	4912	STS-2
ST30	33.0292	88.8548	4958	STS-2
ST33	33.3292	88.8310	5039	STS-2
ST34	33.4086	88.7647	4991	STS-2
ST35	33.4791	88.7369	4934	STS-2
ST36	33.5235	88.6013	5070	STS-2
ST37	33.6076	88.5233	5168	STS-2
ST38	33.6558	88.5043	5070	STS-2
ST39	33.7662	88.3996	5074	STS-2
ST40	33.8165	88.3073	4963	STS-2
NYMA	31.7827	87.3852	4644	STS-2
SANG2	31.0221	91.7001	4714	STS-2
DONG	31.979	90.9126	4607	STS-2

Tabelle A.3: Liste der Stationen des PASSCAL-Teilexperimentes. Alle Stationen waren mit Seismometern vom Typ Streckeisen STS-2 ausgestattet.

Anhang B

Im Rahmen der vorliegenden Arbeit entstandene Publikationen

GEOPHYSICAL RESEARCH LETTERS, VOL. 27, NO. 16, PAGES 2357-2360, AUGUST 15, 2000

Lithospheric and upper mantle structure of the Indian Shield, from teleseismic receiver functions

Joachim Saul

GeoForschungsZentrum Potsdam (GFZ), Potsdam, Germany

M. Ravi Kumar, Dipankar Sarkar

National Geophysical Research Institute, Hyderabad, India

Abstract. Receiver functions derived from teleseismic P waveforms of 297 earthquakes recorded at broadband station Hyderabad (HYB) are analysed to investigate the lithospheric and upper mantle structure in the vicinity of the station, located in the northeastern part of the Archaean Dharwar Craton. The internal structure of the 33±2 km thick crust is simple. It can be approximated by a single layer with S velocity linearly increasing with depth from 3.4 to 4.0 km/s, the average being 3.7±0.2 km/s. The crustal Poisson's ratio is 0.25±0.01. A seismic discontinuity at 90 km depth is inferred from a signal particularly prominent on the SH component and possibly indicative of a layer of depth-localized anisotropy in the lithospheric mantle. The two principal mantle discontinuities are at depths of 406 and 659 km, which are close to the global averages.

Introduction

The large amount of teleseismic data that has accumulated world-wide since the installation of the first digital broadband stations, provides a data base for resolving the deep structure of Earth's interior at ever finer scales. Sophisticated stacking techniques have enabled investigators to gain new knowledge about global 1-D as well as regional 3-D structure. Of particular interest is the structure of the upper mantle and the topography of its most prominent discontinuities, as well as the eventual existence of additional, though possibly not global interfaces within the mantle [*Hales*, 1969; *Shearer*, 1990; *Bostock*, 1996]. In this paper we investigate the stratigraphy of the crust and, for the first time, upper mantle beneath the central Indian Shield using teleseismic P waves recorded at GEOSCOPE station Hyderabad (HYB), the only FDSN station currently operating in India. The STS-1 broadband seismometer is situated directly on Archaean granites in the northeastern part of the Dharwar Craton, which is considered to be the oldest (≈2.6 Ga) and most stable part of the peninsular shield. The relatively simple geotectonic setting provides an excellent condition to image the upper mantle, since signals from deeper discontinuities presumably remain relatively undisturbed by shallow structures.

Few deep seismic sounding surveys have been carried out in the area. None of the lines are closer than 200 km from HYB, and the interpretations have mainly been restricted to the crust [*Kaila and Krishna*, 1992]. More recently, *Gaur and Priestley* [1997] applied receiver function analysis to HYB data, but inverted only two traces. The present study is based on a large number of recordings, permitting a high degree of stacking in the slowness domain. Therefore, not only a reliable crustal model for this still sparsely sampled region is obtained, but also new knowledge of the mantle structure of the Indian Shield.

Paper number 1999GL011128.
0094-8276/00/1999GL011128$05.00

Data and Method

In this study we analyse P waves of 297 earthquakes recorded at HYB in the time period 1989-97 at distances between 30 and 100°. The epicenter distribution is shown in Figure 1. In receiver function analysis, P-to-S converted phases are isolated using component rotation, while deconvolution removes source effects from the waveforms [*Langston*, 1979; *Owens et al.*, 1984; *Ammon*, 1991]. In order to decompose the P, SV and SH wavefields, we rotate the coordinate axes from Z,N,E to ray coordinates L,Q,T [*Vinnik*, 1977; *Kind et al.*, 1995; *Bostock*, 1998] prior to frequency-domain deconvolution. Rotation within the vertical plane (i.e. from Z,R to L,Q) requires knowledge about the polarization angle of the P wave at the receiver. Under the assumption of a laterally homogeneous structure, this angle is a function of the horizontal slowness of the wave and the near-surface S velocity beneath the station [*Ammon*, 1991]. This velocity provides an important constraint to reduce the nonuniqueness of velocities/depths [*Ammon et al.*, 1990] in a subsequent receiver function modelling. It can be determined from the waveforms themselves by measuring the amplitude, at zero delay time, of the direct P phase, which is usually the dominant pulse in R component receiver functions [*Ammon*, 1991]. The result of such a measurement for station HYB is shown in Figure 2. The average value is 3.38 ± 0.16 km/s and is used for the wavefield decomposition.

Receiver functions do not only depend on the S velocity structure, but are also highly sensitive to Poisson's ratio σ [*Zandt and Ammon*, 1995]. The crustal average of σ is determined through comparison of the delay times of the Moho conversion P_Ms and multiples Pp_Ms and Ps_Ms. It is therefore essential that all these phases have sufficiently large amplitudes to permit reliable time measurements. This condition is well met for station HYB, as shown in Figure 3. Delay time curves are drawn for four different σ values. Almost all maxima of both Pp_Ms and Ps_Ms are between the 0.24 and 0.26 curves, and most are even well centered between them, leading to an estimation for σ of 0.25±0.01.

The absence of significant energy preceding the Moho converted phase and large amplitude Moho multiples suggest

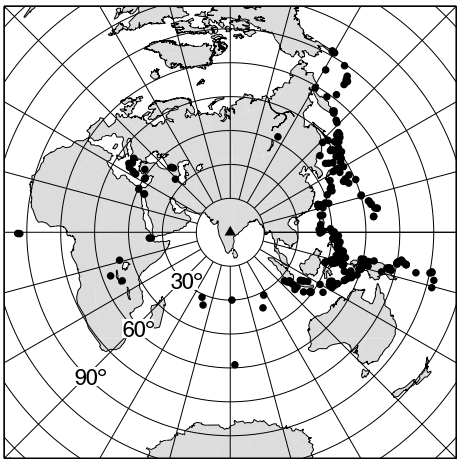

Figure 1. Distribution of events used in this study. The equidistant projection shows the true distances and back-azimuths of the epicenters with respect to HYB.

a very simple crustal structure beneath HYB. This enables us to determine a crustal model through forward-modelling of the P_{MS}, Pp_{MS} and Ps_{MS} delay times and amplitudes. In order to reduce the nonuniqueness of velocities and depths [*Ammon et al.*, 1990], we calibrate the velocities using the previously measured near-surface value of 3.38 km/s. In addition, we assume a sub-Moho velocity of 4.66 km/s, which is the global average reported by *Molnar and Oliver* [1969]. The modelling result is shown in Figure 4. A crust with constant velocity gradient and thickness of 33 km explains both the P_{MS} amplitudes and delay times of all Moho phases. If we let Moho be a 2 km thick gradient layer rather than a first-order discontinuity, we significantly improve the fit for the Moho multiples.

Receiver function analysis was originally developed to investigate crust and uppermost mantle, but has turned out to be a powerful tool for imaging structures at least as deep as the mantle transition zone [*Bostock*, 1996]. In Figure 5 we present a moveout-corrected [*Yuan et al.*, 1997] image of the early part of the SV and SH responses at HYB. While the SV response is dominated by the Moho phases P_{MS}, Pp_{MS} and Ps_{MS}, the prominent signal on SH is a negative polarity phase at 10 s, which shows up in the SV response as a weaker positive signal. Due to its horizontal alignment after moveout correction, this signal is clearly identified as a converted phase from an interface at approximately 90 km depth. Its large amplitude on the transversal component suggests that it could be due to an anisotropic and/or a dipping layer, but neither of the possibilities can be ascertained owing to the lack of sufficient data outside the azimuthal range of 40-120°. In Figure 6 the moveout-corrected SV response of the deep upper mantle and transition zone is shown. The most prominent signal is $P_{410}s$ at a delay time of 43.6 s, which can clearly be traced over the whole slowness range. The $P_{660}s$ phase at 67.8 s, in contrast, appears disrupted due to interference with signals other than P_{DS} conversions. In the averaged trace, however, it stands out clearly, even though it is not as sharp as $P_{410}s$. The $P_{410}s$ and $P_{660}s$ delay times correspond to conversion depths of 406 and 659 km, respectively, based on the global velocity model IASP91 [*Kennett and Engdahl*, 1991]. Besides the signals of these two main mantle discontinuities, numerous phases are visible, which due to their moveout and delay times are identified as free-surface multiples of structures in the depth range of about 80-250 km. These phases can have surprisingly large amplitudes and interfere with P_{DS} phases of deeper structures, resulting in reduced clarity of the latter, which is particularly evident in the case of $P_{660}s$.

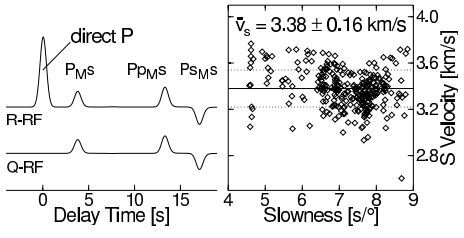

Figure 2. Determination of the near-surface S velocity. The upper trace on the left is a R component synthetic (i.e. after rotation to Z,R). The amplitude of the direct P is a function of slowness and S velocity immediately beneath the station and is used to compute that velocity. Individual measurements for HYB are shown on the right, along with the average (solid line) and standard deviation bounds (dotted lines). Subsequent rotation to L,Q removes the direct P pulse, while retaining the P-to-S converted signals (lower trace).

Discussion and Conclusions

At HYB the average crustal Poisson's ratio of 0.25 is lower than the global average of 0.27 reported by *Zandt and Ammon* [1995], but consistent with measurements of *Last et al.* [1997], who found σ values in the range of 0.24-0.26 for the Tanzania Craton. It remains to be seen whether such relatively low values are generally characteristic for Precambrian shields.

We have found the Moho at HYB to be a pronounced boundary at 33 km depth. Results from a 600 km long wide-

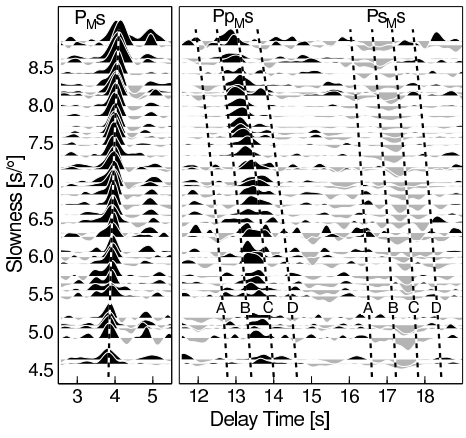

Figure 3. Determination of average crustal Poisson's ratio at HYB. The slowness section was generated by averaging the traces within slowness bins of 0.1 s/° width. Only the time windows covering the Moho phases P_{MS}, Pp_{MS} and Ps_{MS} are shown, with theoretical delay time curves for four different ratios: 0.28 (A), 0.26 (B), 0.24 (C) and 0.22 (D).

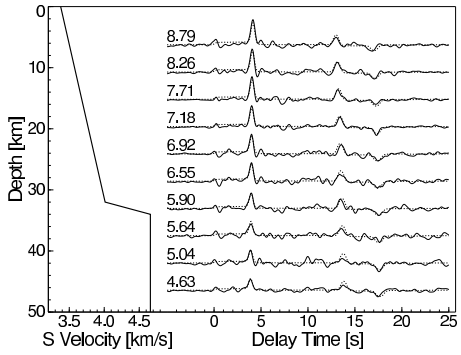

Figure 4. Crustal velocity model for HYB (left). The receiver function stacks used for the forward-modelling were computed by averaging all available traces within 10 slowness bins and are drawn as solid lines, together with the average slowness of each bin in s/°. For comparison, synthetics of the solution model are drawn as dotted lines for each average slowness (right).

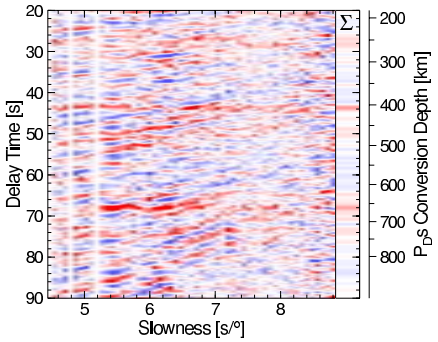

Figure 6. SV response of the upper mantle and transition zone beneath HYB. The response was generated as for Figure 5 and the average over all slownesses is shown on the right.

angle profile, crossing the peninsular shield in E-W direction about 300 km south of Hyderabad, indicate crustal thicknesses varying between 35 and 42 km. Moho depths from other DSS surveys, mostly near the northern margin of the shield, are between 37 and 45 km [see review of *Kaila and Krishna,* 1992]. These values are, however, more representative of tectonically reactivated Proterozoic provinces, rather than of stable Archaean crust. Our study unambiguously brings out a shallower Moho, as also proposed by *Gaur and Priestley* [1997], who deduced slightly higher velocities and consequently a deeper Moho (35 km), but did not explicitly introduce boundary conditions like the near-surface velocity. Even if we increase the average crustal velocity by 5 %, which would correspond to the upper bound of our measurement of the near-surface velocity, we do not get a Moho deeper than 35 km. Furthermore, such an increase of average crustal velocity would also require an unusually high sub-Moho S velocity of about 4.9 km/s, in order to explain the observed P_{MS}. amplitudes. Apparently, the Archaean part of the shield, where Hyderabad is located, has a thinner crust than the Proterozoic belts, where most of the DSS results come from. In this respect our result may conform with the findings of *Durrheim and Mooney* [1991, 1994] namely, that Archaean crust, lacking a high-velocity basal layer, tends to be thinner than Proterozoic crust.

The presence of a seismic discontinuity in the subcrustal lithosphere at 90 km depth has not been reported for India previously. While we have shown the existence of an interface, the origin of the observed energy on SH remains unclear. However, a similar signature under the Slave Craton in Canada, interpreted as an anisotropic layer [*Bostock*, 1998], suggests that the signal more probably represents an effect of depth-localized anisotropy than that of lateral heterogeneities.

The depths of the 410 and 660-km mantle discontinuities are close to the global averages. Nevertheless, the 660 appears to be less sharp than the 410, which could be a structural effect, or due to interference with multiples from shallow mantle structures. No evidence is found for a discontinuity around 520 km depth.

We finally want to request caution when interpreting signal shapes or delay times of mantle P_{DS} phases based on

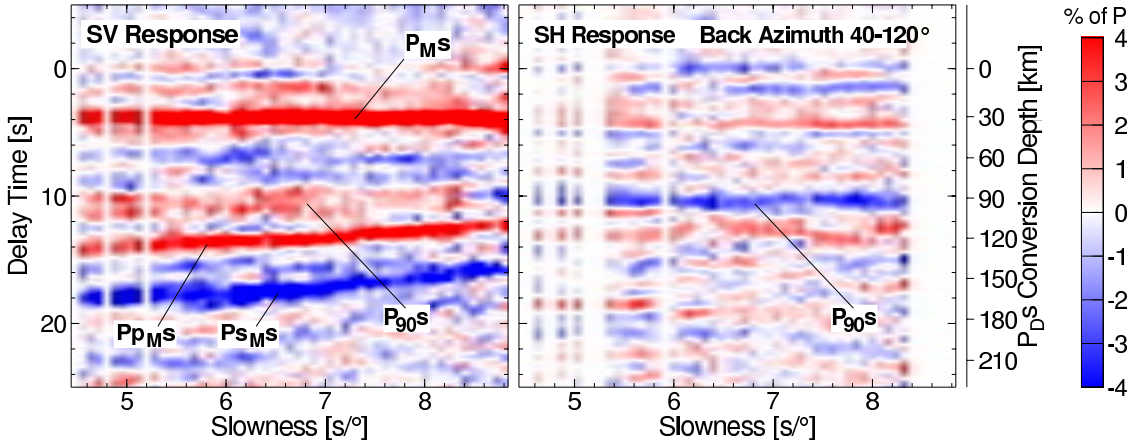

Figure 5. SV (left) and SH (right) responses of crust and shallow upper mantle beneath HYB. The responses were generated by averaging the traces within narrow slowness bins and subsequent moveout correction, the latter resulting in horizontally aligned P_{DS} conversions (i.e. parallel to the slowness axis) in contrast to inclined multiples. The P_{DS} delay times and conversion depths correspond to a slowness of 6.4 s/° (distance of 67°).

single traces or stacks over narrow slowness ranges. Interference with multiples may cause signal distortion and result in misleading conclusions e.g. about the topography or physical nature of discontinuities.

Acknowledgments. We thank Harsh K. Gupta, director of NGRI, and Seweryn J. Duda, Hamburg, for constant encouragement and support. We also thank Rainer Kind, James Ni, Günter Bock and James Mechie for helpful comments on our results. This work was performed under the Indo-German agreement on scientific cooperation administered by the Council of Scientific and Industrial Research, New Dehli, and the Deutsche Forschungsanstalt für Luft- und Raumfahrt e.V., Bonn, who have provided financial support. JS has also been supported by the Deutsche Forschungsgemeinschaft. All figures were produced using the GMT software package [*Wessel and Smith*, 1991].

References

Ammon, C.J., G.E. Randall, and G. Zandt, On the nonuniqueness of receiver function inversions, *J. Geophys. Res., 95,* 15123-15127, 1990.

Ammon, C.J., The isolation of receiver effects from teleseismic P waveforms, *Bull. Seismol. Soc. Am., 81,*, 2504-2510, 1991.

Bostock, M.G., A seismic image of the upper mantle beneath the North American craton, *Geophys. Res. Lett., 23,* 1593-1596, 1996.

Bostock, M.G., Mantle stratigraphy and evolution of the Slave province, *J. Geophys. Res., 103,* 21183-21200, 1998.

Durrheim, R.J., and W.D. Mooney, Archaean and Proterozoic crustal evolution: Evidence from crustal seismology, *Geology, 19,* 606-609, 1991.

Durrheim, R.J., and W.D. Mooney, The evolution of the precambrian lithosphere: Seismological and geochemical constraints, *J. Geophys. Res., 99,* 15359-15374, 1994.

Gaur, V.K., and K.F. Priestley, Shear wave velocity structure beneath the Archaean granites around Hyderabad, inferred from receiver function analysis, *Proc. Indian Acad. Sci., 106,* 1-8, 1997.

Hales, A.L., A seismic discontinuity in the lithosphere, *Earth Planet. Sci. Lett., 7,* 44-46, 1969.

Kaila, K.L., and V.G. Krishna, Deep seismic sounding studies in India and major discoveries, *Curr. Sci., 62,* 117-154, 1992.

Kennett, B.L.N., and E.R. Engdahl, Traveltimes for global earthquake location and phase identification, *Geophys. J. Int.*, *105,* 429-465, 1991.

Kind, R., G.L. Kosarev, and N.V. Petersen, Receiver functions at the stations of the German Regional Seismic Network (GRSN), *Geophys. J. Int.*, *121,* 191-202, 1995.

Langston, C.A., Structure under Mount Rainier, Washington, inferred from teleseismic body waves, *J. Geophys. Res., 84,* 4749-4762, 1979.

Last, R.J., A.N. Nyblade, C.A. Langston, and T.J. Owens, Crustal structure of the East African Plateau from receiver functions and Rayleigh wave phase velocities, *J. Geophys. Res., 102,* 24469-24483, 1997.

Molnar, P., and J. Oliver, Lateral variations of attenuation in the upper mantle and discontinuities in the lithosphere, *J. Geophys. Res., 74,* 2648-2682, 1969.

Owens, T.J., G. Zandt, and S.R. Taylor, Seismic evidence for an ancient rift beneath the Cumberland plateau, Tennessee: a detailed analysis of broadband P waveforms, *J. Geophys. Res., 89,* 7783-7795, 1984.

Shearer, P.M., Seismic imaging of upper mantle structure with new evidence for a 520-km discontinuity, *Nature, 344,* 121-126, 1990.

Vinnik, L.P., Detection of waves converted from P to SV in the mantle, *Phys. Earth Planet. Inter., 15,* 39-45, 1977.

Wessel, P., and W.H.F. Smith, Free software helps map and display data, *Eos Trans. AGU, 72,* 441, 445-446, 1991.

Yuan, X., J. Ni, R. Kind, J. Mechie, and E. Sandvol, Lithospheric and upper mantle structure of southern Tibet from a seismological passive source experiment, *J. Geophys. Res., 102,* 27,491-27,500, 1997.

Zandt, G., and C.J. Ammon, Continental crust composition constrained by measurements of crustal Poisson's ratio, *Nature, 374,* 152-154, 1995.

J. Saul, GeoForschungsZentrum Potsdam (GFZ), Telegrafenberg, 14473 Potsdam, Germany. (e-mail: saul@gfz-potsdam.de)

M.R. Kumar, D. Sarkar, National Geophysical Research Institute, Uppal Road, Hyderabad 500 007, India. (e-mail: postmast@csngri.ren.nic.in)

October 19, 1999; revised March 10, 2000; accepted May 8, 2000.

GEOPHYSICAL RESEARCH LETTERS, VOL. 28, NO. 7, PAGES 1339-1342, APRIL 1, 2001

Crustal structure of the Indian Shield: New constraints from teleseismic receiver functions

M. Ravi Kumar[1], Joachim Saul[2], Dipankar Sarkar[1], Rainer Kind[2], Anshu K. Shukla[3]

Abstract. Teleseismic earthquake waveform data from 10 broadband stations spread over the Indian shield and in operation since 1997, were analyzed to infer the crustal structure, using the receiver function technique. The South Indian shield is characterized by a 33-39 km thick, and remarkably simple crust, with an average Poisson's ratio close to 0.25. The Archaean crust is devoid of any prominent intra-crustal discontinuities. The velocity contrast at the well developed Moho is large, resulting in very clear P-to-S conversions as well as first-order multiples. In contrast, the predominantly Proterozoic crust in the northern part of the shield exhibits a complex character, due to the presence of additional seismic discontinuities. Moho conversions, which are considerably weaker compared to the Archaean terrains, indicate crustal thicknesses of more than 40 km.

Introduction

The Indian shield is a mosaic of various Precambrian tectonic provinces, ranging in age from early Archaean to late Proterozoic. Archaean rocks occur predominantly in the Dharwar craton in the south, the Singhbum craton in the east, the Bundelkhand and Bastar cratons in the center and as relatively small patches in the north-western Aravalli craton. Sedimentation in Aravalli, Singbhum and Cuddapah and the Eastern Ghat orogen took place during the late Proterozoic. The NNE trending, 100-200 km wide, Eastern Ghat mobile belt experienced high grade metamorphism in the late Proterozoic, when it finally accreted to the Indian shield [*Naqvi and Rogers*, 1996]. A region of massive Cretaceous flood basalts, the Deccan Volcanic Province (DVP), is a conspicuous geological feature in the western part of the Indian shield. The ENE trending Narmada-Son Lineament (NSL), believed to have formed during middle to late Archaean [Radhakrishna, 1989] and subsequently reactivated during the Proterozoic, serves as a tectonic boundary between the southern peninsular block and the northern foreland block.

Estimates of the crustal thickness in the Indian region have been obtained primarily through Deep Seismic Sounding (DSS) studies [*Kaila and Krishna*, 1992]. The uppermost mantle P velocities in the subcontinent range from 7.9 to 8.6 km/s. However, the crustal models obtained through earlier DSS experiments have limited resolution due to the narrow frequency band of analog data and uncertainties inherent in travel time modelling of wide angle reflections. For this study, we utilise broadband data from a recently installed network of 10 stations to model the crustal structure beneath each station, using the receiver function method [*Langston*, 1979; *Owens et al.*, 1984]. This technique isolates P-to-S converted phases from the coda of teleseismic P waves through component rotation, and source-side effects are equalized by subsequent deconvolution. This technique is now commonly used to investigate the crust and upper mantle structure.

Data and Method

In 1997, the India Meteorological Department (IMD) upgraded 10 of its seismological observatories to the standards of Global Seismological Networks (GSN), to specifically monitor the Indian shield seismicity. The IMD stations, all equipped with STS-2 broadband sensors, are distributed on various tectonic provinces within the Indian Shield (Figure 1). Stations KARD, PUNE, BLSP and MDRS are situated in regions with Archaean crystalline basement. While

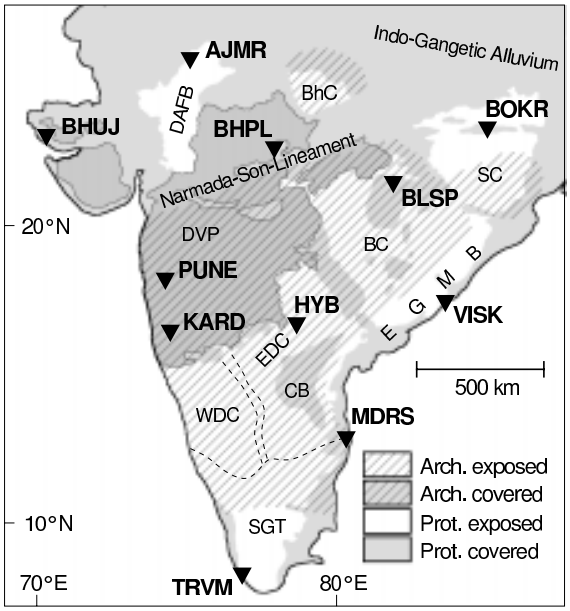

Figure 1. Geological map of the Indian shield showing age and exposure of the Precambrian basement and the locations of the broadband stations. This map is simplified after *Goodwin* [1996] and some Proterozoic terrains contain small patches of Archaean crust. SGT: Southern Granulite Terrain; WDC: Western Dharwar Craton; EDC: Eastern Dharwar Craton; EGMB: Eastern Ghat Mobile Belt; DVP: Deccan Volcanic Province; BC: Bhandara Craton; SC: Singhbum Craton; BhC: Bundelkhand Complex; DAFB: Delhi Aravalli Fold Belt

[1]National Geophysical Research Institute, Hyderabad, India
[2]GeoForschungsZentrum Potsdam (GFZ), Potsdam, Germany
[3]India Meteorological Department, New Delhi, India

Paper number 2000GL012310.
0094-8276/01/2000GL012310$05.00

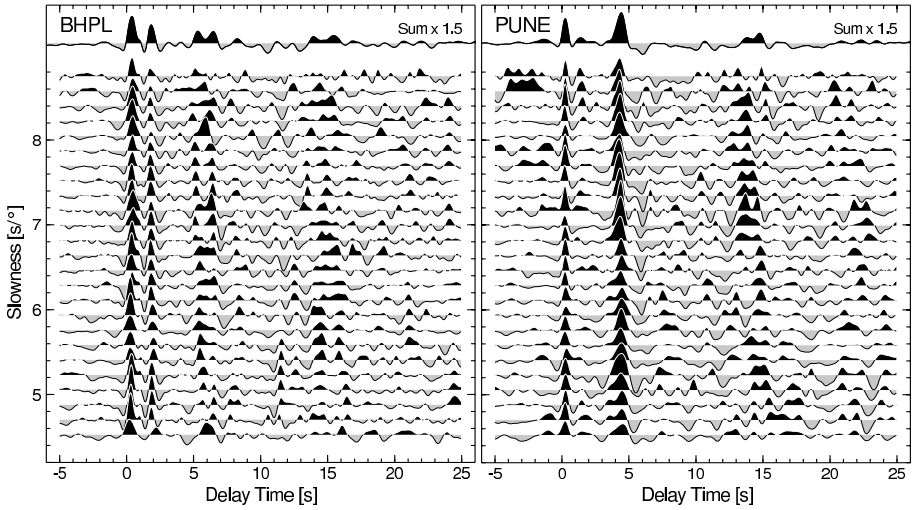

Figure 2. Raw receiver functions for BHPL and PUNE averaged over narrow slowness bins. The average of all the traces is shown at the top.

at KARD and PUNE the basement is covered by the Deccan traps, BLSP lies in the Proterozoic Chattisgarh basin, within the Archaean Bhandara craton. At MDRS high grade metamorphic rocks are exposed. The basement rocks in the vicinities of stations BHPL, VISK, TRVM, AJMR, BHUJ and BOKR are of Proterozoic age. BHPL is located within the DVP, where the traps are underlain by Paleozoic sediments with an early Proterozoic basement. VISK is situated on the Eastern Ghat Mobile Belt, whereas TRVM, near the southern tip of the subcontinent, lies in the presumably Proterozoic part of the Southern Granulite Terrain (SGT). Station AJMR is located in the Proterozoic Delhi-Aravalli fold belt (DAFB), BHUJ within the Mesozoic Kutch sedimentary basin, and BOKR within the Proterozoic northern half of the Singhbum craton.

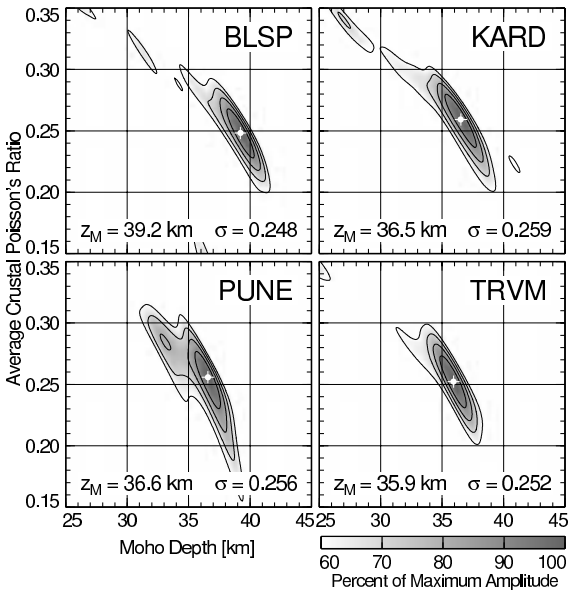

Figure 3. Measurements of the Poisson's ratios (σ) and Moho depths (z_M) for four IMD stations.

For the present study, nearly 3 years of teleseismic data were available. The number of usable recordings per station varied significantly, ranging from more than a hundred for stations BHPL, KARD, PUNE and VISK to just four in the case of BLSP (Tab. 1). The decomposition of the P wave coda into P, SV and SH components requires knowledge of the near-surface velocity at each station [*Bostock*, 1998], which we obtain using the technique of *Saul et al.* [2000]. The receiver functions are computed using spectral division, with a Gaussian parameter of 4 Hz. A moveout correction for P-to-S converted phases is applied to account for the slowness dependence of arrival times, by adjusting the times to the slowness value of 6.4 s/°. This aligns the P_MS phase parallel to the slowness axis, when plotted against slowness. Multiples, on the other hand, become more inclined with respect to the slowness axis, due to their opposite moveout. Thus the moveout-correction and subsequent stacking focus converted phases [*Yuan et al.*, 1997]. Figure 2 illustrates the SV responses for stations BHPL and PUNE, obtained by averaging the individual receiver functions in narrow slowness bins.

In order to quantify the crustal structure, we prefer simple forward modelling to the inversion procedure normally adopted. Instead of attempting to match every single wiggle in a trace, only those features that are coherent across most of the records (Figure 2) are modelled. This usually results in simpler models compared to those obtained from inversion, which often produces complicated models. Although the forward approach may be considered subjective, the good waveform fit, which is often achieved, justifies this approach. Prior to the actual forward modelling, we estimate the average crustal Poisson's ratio σ and Moho depth z_M following the approach of *Zhu and Kanamori* [2000]. This technique involves a grid search over the σ- z_M space, to determine the (σ, z_M) pair which is in closest agreement with the observed P_MS, Pp_MS and Ps_MS waveforms. Therefore, this method requires the presence of clear Moho multiples.

Table 1. Summary of main crustal parameters

Station	lat. °	lon. °	no. obs.	τ_M s	σ	$\overline{v}_s$ km/s	Z_M km
AJMR	26.5	74.6	58	3.4?	-	-	29?
BHPL	23.2	77.4	183	5.4	-	3.85	46
BHUJ	23.3	69.7	39	5.2	-	-	44
BLSP	22.1	82.1	4	4.7	0.248	3.75	39.2
BOKR	23.8	85.9	28	6.3?	-	-	54?
KARD	17.3	74.2	130	4.4	0.259	3.7	36.5
MDRS	13.1	80.2	23	4.4	-	3.8	38
PUNE	18.5	73.8	163	4.4	0.257	3.7	36.5
TRVM	8.5	77.0	56	4.3	0.254	3.7	35.9
VISK	17.7	83.3	129	4.0	-	3.75	35

Results

The main results of this study are summarized in Table 1. Poisson's ratio could be determined only for stations BLSP, KARD, PUNE, and TRVM (Figure 3), due to the lack of clear Moho multiples at all other stations. The receiver functions for the stations KARD, MDRS, PUNE and TRVM, i.e. those within the South Indian shield, are dominated by large-amplitude Moho conversions at delay times of about 4.4 s (Figure 4), indicating pronounced velocity contrasts at depths of 36-38 km (Figure 5). Further, rather uniform Poisson's ratios close to 0.25 are obtained. At PUNE, a moderate velocity inversion appears to be present in the mantle at 53 km depth, producing a prominent negative phase at 6.2 s (Figure 2). At BLSP the custal thickness is 39 km, with an average Poisson's ratio of 0.25 also. In addition to the Moho, a prominent mid-crustal boundary is present at about 26 km depth. The crustal models for stations VISK and BHPL deviate significantly from the above simple structures. At BHPL, a clear conversion at 1.8 s is indicative of a pronounced mid-crustal boundary. Coherent arrivals are also observed at 5.4 and 6.5 s. Either of them could be the Moho conversion, with the other being a multiple from the shallower interface. The receiver functions have therefore been modelled considering both possibilities, with Moho depths of 46 and 55 km, respectively. The model with a deeper Moho, however, requires a very high Poisson's ratio of 0.31 for the upper crust. We therefore prefer the model with a shallower Moho. At VISK, lateral heterogeneities produce a large azimuthal variation in the RF's which are, however, not quantifiable due to insufficient azimuthal coverage. A 1-D modelling yields two prominent discontinuities at depths of 35 and 52 km. While the S velocity at 35 km is found to be 4.3 km/s, a velocity greater than 4.6 km/s is reached only at 52 km. At AJMR, the only candidate for P_MS is at 3.5 s, corresponding to a crustal thickness of 29 km. In spite of the good quality receiver functions for station BHUJ, no clear Moho signature is visible. A strong, broad phase at about 0.7 s is associated with the basement underneath the shallow, very low velocity ($v_s = 1.2$ km/s) sediments, multiples of which probably mask later conversions. However, a weak phase at about 5.2 s could be interpreted as the Moho, at a depth of 44 km. The structure at BOKR in eastern India appears complicated. The individual receiver functions exhibit a complex behaviour, varying strongly with azimuth. A phase at 6.3 s is most likely the P_MS conversion, as it is the only azimuthally consistent signal. This would correspond to a Moho depth of about 54 km, assuming an average S velocity of 3.7 km/s.

Discussion

The present study has brought out the crustal structure at various locations in the Indian shield. The crustal thickness of 36 km below PUNE and KARD is identical to that inferred from wide-angle reflection studies [*Krishna et al.*, 1989] near KARD. Moho depths of 35-37 km have also been reported from the Latur region, on the eastern fringe of trap covered shield [*Krishna et al.*, 1999]. The crust at PUNE and KARD is very simple and similar to that at HYB, situated on the Archaean basement outside the DVP, about 500 km to the east [*Saul et al.*, 2000], indicating that the massive extrusion of Deccan basalts has not significantly affected the underlying crust. The high surface S velocity of 3.75 km/s at MDRS and TRVM is consistent with the generally high velocities of mafic granulites. The Moho at MDRS is slightly deeper than at KARD and PUNE, in agreement with the higher average crustal velocity and thus reduced velocity contrast across the Moho required by the significantly lower P_MS amplitude.

The crustal thickness of 46 km from the preferred model for BHPL disagrees with a previous wide-angle study 40 km W of BHPL [*Kaila and Rao.*, 1986], which indicated a shallower (35-40 km) Moho. However, neglection of a high P

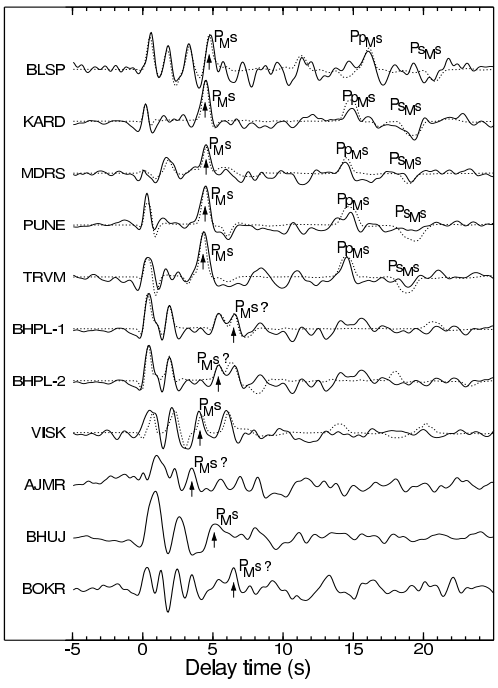

Figure 4. Observed receiver functions stacks (solid line), together with the synthetics (dotted lines) corresponding to the models in Fig. 5. The Moho P-to-S conversion P_MS and multiples PP_MS and Ps_MS are indicated. BHPL-1 represents the deep Moho model and BHPL-2, the shallow one. Modelling is not attempted for stations BHUJ, BOKR and AJMR, due to complexity of RF's.

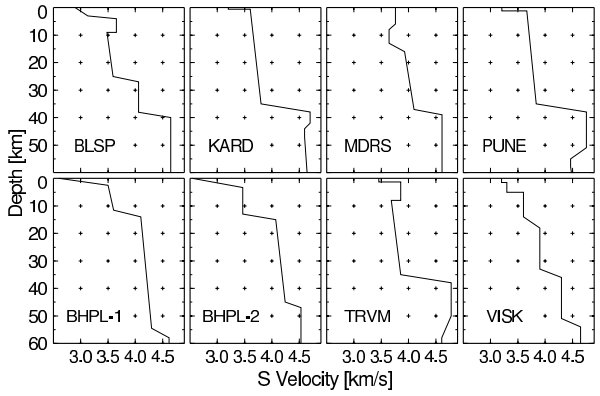

Figure 5. Shear wave velocity models beneath the stations indicated. Two alternative models are shown for station BHPL.

velocity (≈6.7 km/s) at about 5 km depth [*Kumar et al.*, 2000], may have resulted in too shallow a Moho. Beneath VISK, either of the two discontinuities could be the Moho. Given the geological history of continental rifting along the eastern margin, a partial reworking of the crust at VISK appears probable and therefore a classification in terms of crustal age is likely to fail. We interpret the interface at 35 km as the Moho, with the high-velocity layer beneath being the result of Phanerozoic underplating. At AJMR, associating the interface at 29 km with the Moho is questionable, in view of the 13 s TWT reported for Moho reflections observed 50 km east of AJMR, indicating a depth close to 40 km [*Rajendra Prasad et al.*, 1998]. Alternatively, the interface at 29 km may represent the top of a high-velocity layer at the base of the crust with too low a velocity contrast to the mantle to generate a prominent P-to-S conversion. The similiarity of the structure at TRVM to the Archaean localities in the peninsular shield indicates the need for a careful examination of its classification as Proterozoic.

A general inference from this study is that the Archaean terrains of the South Indian Shield are characterized by a remarkably simple and uniform crustal structure, with the Moho being consistently shallower than 40 km. The Proterozoic crust, in contrast, is complicated with the presence of at least one mid-crustal discontinuity and a clear tendency towards larger thicknesses, in most cases more than 40 km. This thus appears to follow the global trend reported by *Durrheim and Mooney* [1994] that Archaean is thinner than Proterozoic crust. We anticipate that analysis of broadband data from additional stations that are being installed on the Indian shield, as well as temporary deployments, will soon enable us to resolve this issue more conclusively.

Acknowledgments. This study was performed under the DLR-CSIR scientific collaboration project No. IND/0013. JS has also been supported by the Deutsche Forschungsgemeinschaft. H.K. Gupta and S.J. Duda have rendered continuous support for this study. We sincerely thank D.S. Ramesh, Larry Brown, Jim Mechie, R. Srinivasan, N. Purnachandra Rao and an anonymous reviewer for useful discussions and thorough review of the manuscript.

References

Bostock, M.G., Mantle stratigraphy and evolution of the Slave province, *J. Geophys. Res., 103,* 21183-21200, 1998.

Durrheim, R.J., and W.D. Mooney, The evolution of the precambrian lithosphere: Seismological and geochemical constraints, *J. Geophys. Res., 99,* 15359-15374, 1994.

Goodwin, A.M., Principles of Precambrian Geology, Academic press, London, 327pp., 1996.

Kaila, K.L., and P. Koteswara Rao, Crustal structure along Khajuriakalam-Rahatgaon-Betul-Multai-Pulgaon profiles across the Narmada lineament from deep seismic soundings, in: Deep seismic soundings and Crustal tectonics, Ed: K.L. Kaila and H.C. Tewari, AEG publication Hyderabad, 43-59, 1986.

Kaila, K.L., and V.G. Krishna, Deep seismic sounding studies in India and major discoveries, *Curr. Sci., 62,* 117-154, 1992.

Krishna, V.G., K.L. Kaila, and P.R. Reddy, Synthetic seismogram modelling of crustal seismic record sections from the Koyna DSS profiles in the western India, in Properties and processes of the lower crust, Eds: R.F. Mereu, S. Mueller and D.M. Fountain, Geophysical Monograph 51, AGU/IUGG publication, 6, 143-157, 1989.

Krishna, V.G., C.V.R.K. Rao, H.K. Gupta, D. Sarkar, and M. Baumbach, Crustal seismic velocity structure in the epicentral region of Latur earthquake (September 29, 1993), Southern India: Inferences from modelling of the aftershock seismograms, *Tectonophys., 304,* 241-255, 1999.

Kumar, P., H. C. Tewari, and G. Khandekar: An anomalous high-velocity layer at shallow crustal depths in the Narmada zone, India, *Geophys. J. Int., 142,* 95-107, 2000.

Langston, C.A., Structure under Mount Rainier, Washington, inferred from teleseismic body waves, *J. Geophys. Res., 84,* 4749-4762, 1979.

Naqvi, S.M., and J.J.W. Rogers, Precambrian Geology of India, Clarendon press, New York, 1996.

Owens, T.J., G. Zandt, and S.R. Taylor, Seismic evidence for an ancient rift beneath the Cumberland Plateau, Tennessee, *J. Geophys. Res., 116,* 618-636, 1984.

Radhakrishna, B.P., Suspect Tectono-stratigraphic terrane elements in the Indian subcontinent,*J. Geol. Soc. India, 34,* 1-24, 1989.

Rajendra Prasad, B., H.C. Tewari, V. Vijay Rao, M.M. Dixit, and P.R. Reddy, Structure and tectonics of the Proterozoic Aravalli-Delhi Fold Belt in northwestern India from deep seismic reflection studies, *Tectonophys., 288,* 31-41, 1998.

Saul, J., M.R. Kumar, and D. Sarkar, Lithospheric and upper mantle structure of the Indian Shield, from teleseismic receiver functions, *Geophys. Res. Lett., 27,* 2357-2360, 2000.

Yuan, X., J. Ni, R. Kind, J. Mechie, and E. Sandvol, Lithospheric and upper mantle structure of southern Tibet from a seismological passive source experiment, *J. Geophys. Res., 102,* 27,491-27,500, 1997.

Zhu, L. and H. Kanamori, Moho depth variation in southern California from teleseismic receiver functions, *J. Geophys. Res., 105,* 2969-2980, 2000.

M.R. Kumar, D. Sarkar, National Geophysical Research Institute, Uppal Road, Hyderabad 500 007, India.(e-mail: postmast@csngri.ren.nic.in)

J. Saul, R. Kind, GeoForschungsZentrum Potsdam (GFZ), Telegrafenberg, 14473 Potsdam, Germany. (e-mail: saul@gfz-potsdam.de)

A.K. Shukla, India Meteorological Department, Lodhi Road, New Delhi, India.

(Received September 7, 2000; revised December 12, 2000; accepted December 20, 2000.)

Literaturverzeichnis

Allegre, C. J., Courtillot, V., Tapponnier, P., und 33 others, Structure and evolution of the Himalaya-Tibet orogenic belt, *Nature*, **307**, 17–22, 1984.

Allegre, C. J., Birck, J. L., Capmas, F., und Courtillot, V., Age of the Deccan traps using ^{187}Re-^{187}Os systematics, *Earth and Planetary Science Letters*, **170**, 157–349, 1999.

Ammon, C. J., The isolation of receiver effects from teleseismic P waveforms, *Bull. Seism. Soc. Am.*, **81**, 2504–2510, 1991.

Ammon, C. J., Randall, G. E., und Zandt, G., On the nonuniqueness of receiver function inversions, *J. Geophys. Res.*, **95**, 15 303–15 318, 1990.

Argand, E., La tectonique de l'Asie, *Proc. 13th Int. Geol. Congr.*, pp. 170–372, 1924.

Barazangi, M. und Ni, J., Velocities and propagation characteristics of Pn and Sn beneath the Himalayan arc and Tibetan plateau: Possible evidence for underthrusting of Indian continental lithosphere beneath Tibet, *Geology*, **10**, 179ff., 1982.

Bina, C. R. und Helffrich, G. R., Phase transition Clapeyron slopes and transition zone seismic discontinuity topography, *J. Geophys. Res.*, **99**, 15,853–15,860, 1994.

Bird, P. und Toksöz, M. N., Strong attenuation of Rayleigh waves in Tibet, *Nature*, **266**, 161–163, 1977.

Blisniuk, P. M., Hacker, B. R., Glodny, J., Ratschbacher, L., Bi, S., Wu, Z., McWilliams, M. O., und Calvert, A., Crustal thinning in Central Tibet since at least 13.5 Myr., *Nature*, **412**, 628–632, 2001.

Bock, G., Synthetic seismogram images of upper mantle structure: No evidence for a 520-km discontinuity, *J. Geophys. Res.*, **103**, 15 843–15 851, 1994.

Bond, G. C., Nickeson, P. A., und Kominz, M. A., Breakup of a supercontinent between 625 and 555 ma: new evidence and implications for continental histories, *Earth and Planetary Science Letters*, **70**, 325–345, 1984.

Bostock, M. G., Ps conversions from the upper mantle transition zone beneath the Canadian landmass, *J. Geophys. Res.*, **101**, 8393–8402, 1996.

Bostock, M. G., Mantle stratigraphy and evolution of the Slave Province, *J. Geophys. Res.*, **103**, 21.183–21.200, 1998.

Bostock, M. G., Rondenay, S., und Shragge, J., Multi-parameter 2-D inversion of scattered teleseismic body-waves–1. Theory for oblique incidence, *J. Geophys. Res.*, **106**, 30,771–30,782, 2001.

Brown, L. D., Zhao, W., ans M. Hauck, K. D. N., Alsdorf, D., Ross, A., Cogan, M., Clark, M., Liu, X., , und Che, J., Bright spots, structure and magmatism in southern Tibet from INDEPTH seismic reflection profiling, *Science*, **274**, 1688–1690, 1996.

Bruguier, O., Lancelot, J. R., und Malavielle, J., U-Pb dating on single detrital zirkon grains from the Triassic Songpan-Ganze flysch (Central China): Provenance and tectonic correlations, *Earth and Planetary Science Letters*, **152**, 217–231, 1997.

Castle, J. C. und Creager, K. C., Seismic evidence against a mantle chemical discontinuity near 660-km depth beneath Izu-Bonin, *Geophys. Res. Lett.*, **24**, 241–244, 1997.

Chen, W. und Molnar, P., Focal depths of intracontinental and intraplate earthquakes and their implications for the thermal and mechanical properties of the lithosphere, *J. Geophys. Res.*, **88**, 4183–4214, 1983.

Chen, W. P. und Özalaybey, S., Correlation between seismic anisotropy and Bouguer gravity anomalies in Tibet and its implications for lithospheric structure, *Geophys. J. Int.*, **135**, 93–101, 1998.

Chevrot, S., Vinnik, L., und Montagner, J.-P., Global-scale analysis of the mantle Pds phases, *J. Geophys. Res.*, **104**, 20,203–20,219, 1999.

Coleman, M. und Hodges, K., Evidence for Tibetan plateau uplift before 14 Myr ago from a new minimum age for east-west extension, *Nature*, **374**, 49–52, 1995.

Collier, J. D. und Helffrich, G. R., Topography of the “410” and “660” km seismic discontinuities in the Izu-Bonin subduction zone, *Geophys. Res. Lett.*, **24**, 1535–1538, 1997.

DeCelles, P. G., Robinson, D. M., und Zandt, G., Implications of shortening in the Himalayan fold-thrust belt for uplift of the Tibetan Plateau, *Tectonics*, **6**, 1062 ff., 2002.

Dewey, J. F. und Bird, J. M., Mountain belts and the New Global Tectonics, *J. Geophys. Res.*, **75**, 2625–2647, 1970.

Dewey, J. F. und Burke, K. C., Tibetan, Variscan and Pre-Cambrian basement reactivation products of continential collision, *J. Geol.*, **81**, 683–692, 1973.

Dueker, K. G. und Sheehan, A. F., Mantle discontinuity structure from midpoint stacks of converted P to S waves across the Yellowstone hotspot track, *J. Geophys. Res.*, **102**, 8313–8327, 1997.

Dueker, K. G. und Sheehan, A. F., Mantle discontinuity structure beneath the Colorado Rocky Mountains and High Plains, *J. Geophys. Res.*, **103**, 7153–7169, 1998.

Dziewonski, A. M., Chou, T.-A., und Woodhouse, J. H., Determination of earthquake source parameters from waveform data for studies of global and regional seismicity, *J. Geophys. Res.*, **86**, 2825–2852, 1981.

England, P. und Houseman, G., Finite strain calculation of continental deformation, *J. Geophys. Res.*, **91**, 3664–3676, 1986.

Flanagan, M. P. und Shearer, P. M., Global mapping of topography on transition zone velocity discontinuities by stacking SS precursors, *J. Geophys. Res.*, **103**, 2673–2692, 1998.

Frederiksen, A. W. und Bostock, M. G., Modelling teleseismic waves in dipping anisotropic structures, *Geophys. J. Int.*, **141**, 401–412, 2000.

Friederich, W., The S-velocity structure of the East Asian mantle from inversion of shear and surface waveforms, *Geophys. J. Int.*, **153**, 88–102, 2003.

Gansser, A., The significance of the Himalayan suture zone, *Tectonophysics*, **62**, 37–52, 1980.

Godfrey, N. J., Christensen, N. I., und Okaya, D. A., Anisotropy of schists: Contribution of crustal anisotropy to active source seismic experiments and shear wave splitting observations, *J. Geophys. Res.*, **105**, 27,991–28,007, 2000.

Goodwin, A. M., *Principles of Precambrian Geology*, Academic press, London, 1996.

Griot, D.-A., Montagner, J.-P., und Tapponnier, P., Phase velocity structure from Rayleigh and Love waves in Tibet and its neighboring regions, *J. Geophys. Res.*, **103**, 21,215–21,232, 1998.

Gupta, H. K. und Narain, H., Crustal structure of the Himalayan and the Tibetan Plateau regions from surface wave dispersion, *Bull. Seism. Soc. Am.*, **57**, 235–248, 1967.

Gurrola, H., Minster, J., und Owens, T., The use of velocity spectrum for stacking receiver functions and imaging upper mantle discontinuities, *Geophys. J. Int.*, **117**, 427–440, 1994.

Haines, S. S., Klemperer, S. L., Brown, L., Jingru, G., Mechie, J., Meissner, R., Ross, A., , und Wenjin, Z., INDEPTH III seismic data: From surface observations to deep crustal processes in Tibet, *Tectonics*, **22**, 2003.

Hirn, A., Nercessian, A., Sapin, M., Jobert, G., Jin, X., Yuan, G., Jing, W., Yuan, L., und Wen, T., Lhasa block and bordering sutures - a continuation of a 500-km Moho traverse through Tibet, *Nature*, **307**, 25–27, 1984.

Hirn, A. e. a., Seismic anisotropy as an indicator of mantle flow beneath the Himalayas and Tibet, *Nature*, **375**, 571–574, 1995.

Hodges, K. V., Tectonics of the Himalaya and southern Tibet from two perspectives, *Geol. Soc. Am. Bull.*, **112**, 324–350, 2000.

Houseman, G., McKenzie, D. P., und Molnar, P., Convective instability of a thickened boundary layer and its relevance for the thermal evolution of continental convergent belts, *J. Geophys. Res.*, **86**, 6115–6132, 1981.

Huang, W. C., Ni, J. F., Tilmann, F., Nelson, D., Guo, J., Zhao, W., Mechie, J., Kind, R., Saul, J., Rapine, R., und Hearn, T. M., Seismic polarization anisotropy beneath the central Tibetan Plateau, *J. Geophys. Res.*, **105**, 27,979 – 27,989, 2000.

Jackson, J., Strength of the continental lithosphere: Time to abandon the jelly sandwich?, *GSA Today*, **12**, 4–10, 2002.

Kaila, K. L. und Krishna, V. G., Deep seismic sounding studies in India and major discoveries, *Curr. Sci.*, **62**, 117–154, 1992.

Kapp, P., Yin, A., Manning, C. E., Murphy, M., Harrison, T. M., Spurlin, M., Ding, L., Deng, X.-G., und Wu, C.-M., Blueschist-bearing metamorphic core complexes in the Qiantang reveal deep crustal structure of northern Tibet, *Geology*, **28**, 19–22, 2000.

Kennett, B. L. N. und Engdahl, E. R., Travel times for global earthquake location and phase identification, *Geophys. J. Int.*, **105**, 429–465, 1991.

Kind, R., Kosarev, G. L., und Petersen, N. V., Receiver functions at the stations of the German Regional Seismic Network (GRSN), *Geophys. J. Int.*, **121**, 191–202, 1995.

Kind, R., Ni, J., Zhao, W., Wu, J., Yuan, X., Zhao, L., Sandvol, E., Reese, C., Nabelek, J., und Hearn, T., Evidence from earthquake data for a partially molten crustal layer in southern Tibet, *Science*, **274**, 1692–1694, 1996.

Kind, R., Yuan, X., Saul, J., Nelson, D., Sobolev, S., Mechie, J., Zhao, W., Kosarev, G., Ni, J., Achauer, U., und Jiang, M., Seismic images of crust and upper mantle beneath Tibet: Evidence for Eurasian plate subduction, *Science*, **298**, 1219–1221, 2002.

Kosarev, G., Kind, R., Sobolev, S., Yuan, X., Hanka, W., und Oreshin, S., Seismic evidence for a detached Indian lithospheric mantle beneath Tibet, *Science*, **283**, 1306–1309, 1999.

Kumar, M. R., Saul, J., Sarkar, D., Kind, R., und Shukla, A. K., Crustal structure of the Indian Shield: New constraints from teleseismic receiver functions, *Geophys. Res. Lett.*, **28**, 1339–1342, 2001.

Kumar, M. R., Ramesh, D. S., Saul, J., Sarkar, D., und Kind, R., Crustal structure and upper mantle stratigraphy of the Arabian Shield, *Geophys. Res. Lett.*, **29**, 2002.

Langston, C. A., The effect of planar dipping structure on source and receiver responses for constant ray parameter, *Bull. Seism. Soc. Am.*, **67**, 1029–1050, 1977.

Langston, C. A., Structure under Mount Rainier, Washington, inferred from teleseismic body waves, *J. Geophys. Res.*, **84**, 4749–4762, 1979.

Levin, V. und Park, J., P-SH conversions in a flat-layered medium with anisotropy of arbitrary orientation, *Geophys. J. Int.*, **131**, 253–266, 1997.

Li, X., Kind, R., Priestley, K., Sobolev, S. V., Tilman, F., Yuan, X., und Weber, M., Mapping the Hawaiian plume conduit with converted seismic waves, *Nature*, **405**, 938–941, 2000a.

Li, X., Sobolev, S., Kind, R., Yuan, X., und Estabrook, C., A detailed receiver function image of the upper mantle discontinuities in the Japan subduction zone, *Earth and Planetary Science Letters*, **183**, 527–541, 2000b.

Li, X., Kind, R., Yuan, X., Sobolev, S. V., Hanka, W., Ramesh, D. S., Gu, Y., und Dziewonski, A. M., Seismic observation of narrow plumes in the oceanic upper mantle, *Geophys. Res. Lett.*, **30**, 1334–1337, 2003.

Liu, S., *Aeromagnetic anomaly map of China and the adjacent sea areas (1:4 000 000)*, China Cartographic Publishing House, 1989.

Maggi, A., Jackson, J. A., Priestley, K., und Baker, C., A reassessment of focal depth distributions in southern Iran, the Tien Shan and northern India: Do earthquakes really occur in the continental mantle?, *Geophys. J. Int.*, **143**, 629–661, 2000.

Makovsky, Y. und Klemperer, S. L., Measuring the seismic properties of Tibetan bright spots: Evidence for free aqueous fluids in the Tibetan middle crust, *J. Geophys. Res.*, **104**, 10 795–10 825, 1999.

Makovsky, Y., Klemperer, S. L., Ratschbacher, L., und Alsdorf, D., INDEPTH Wide-angle profiling traces mid-crustal reflector: an ophiolitic slab beneath the India-Asia suture in southern Tibet?, *Tectonics*, **18**, 793–808, 1999.

McNamara, D., Owens, T., Silver, P., und F.Wu, Shear wave anisotropy beneath the Tibetan Plateau, *J. Geophys. Res.*, **99**, 13,655–13,665, 1994.

McNamara, D. E. und Owens, T. J., Azimuthal shear wave velocity anisotropy in the Basin and Range province using Moho Ps converted phases, *J. Geophys. Res.*, **98**, 12,003–12,017, 1993.

McNamara, D. E., Owens, T. J., Walter, W. R., und Owens, T. J., Observations of regional phase propagation across the Tibetan Plateau, *J. Geophys. Res.*, **100**, 22,215–22,229, 1995.

McNamara, D. E., Walter, W. R., Owens, T. J., und Ammon, C. J., Upper mantle velocity structure beneath the Tibetan Plateau from Pn travel time tomography, *J. Geophys. Res.*, **102**, 493–505, 1997.

Mechie, J., Sobolev, S. V., Ratschbacher, L., Babeyko, A. Y., Bock, G., Jones, A. G., Nelson, K. D., Solon, K. D., Brown, L. D., und Zhao, W., Precise temperature estimation in the Tibetan crust from seismic detection of the alpha-beta quartz transition, *submitted to Geology*, 2003.

Molnar, P. und Tapponnier, P., Cenozoic tectonics of Asia: effects of a continental collision, *Science*, **189**, 419–426, 1975.

Negi, J., Pandey, O., und Agrawal, P., Supermobility of hot Indian lithosphere, *Tectonophysics*, **131**, 147–156, 1986.

Nelson, K. D., Zhao, W., Brown, L. D., Kuo, J., Che, J., Liu, X., Klemperer, S. L., Makovsky, Y., Meissner, R., Mechie, J., Kind, R., Wenzel, F., Ni, J., Nabelek, J., Leshou, C., Tan, H., Wei, W., Jones, A. G., Booker, J., Unsworth, M., Kidd, W. S. F., Hauck, M., Alsdorf, D., Ross, A., Cogan, M., Wu, C., Sandvol, E., , und Edwards, M., Partially molten middle crust beneath southern Tibet: Synthesis of project INDEPTH results, *Science*, **274**, 1684–1687, 1996.

Ni, J. und Barazangi, M., High-frequency seismic wave propagation beneath the Indian shield, Himalayan arc, Tibetan plateau and surrounding regions: high uppermost mantle velocities and efficient Sn propagation beneath Tibet, *Geophys. J. R. Astr. Soc.*, **72**, 665–689, 1983.

Ni, J. und Barazangi, M., Seismotectonics of the Himalayan collision zone: Geometry of the underthrusting Indian plate beneath the Himalaya, *J. Geophys. Res.*, **89**, 1147–1163, 1984.

Okaya, D. A. und Christensen, N. I., Anisotropic effects of non-axial seismic wave propagation in foliated crustal rocks, *Geophys. Res. Lett.*, **29**, 1507–1510, 2002.

Owens, T. J. und Zandt, G., Implications of crustal property variations for models of Tibetan Plateau evolution, *Nature*, **387**, 37–43, 1997.

Owens, T. J., Zandt, G., und Taylor, S. R., Seismic evidence for an ancient rift beneath the Cumberland Plateau, Tennessee: a detailed analysis of broadband teleseismic P waveforms, *J. Geophys. Res.*, **89**, 7783–7795, 1984.

Patriat, P. und Achache, J., India-Asia collision chronology and implications for crustal shortening and driving mechanism of plates, *Nature*, **311**, 615–621, 1984.

Purnachandra Rao, N., Tsukuda, T., Kosuga, M., Bhatia, S. C., und Suresh, G., Deep lower crustal earthquakes in central India: Inferences from analysis of regional broadband data of the 1997 May 21, Jabalpur earthquake, *Geophys. J. Int.*, **148**, 132–138, 2002.

Radhakrishna, B. P., Suspect tectono-stratigraphic terrane elements in the Indian subcontinent, *J. Geol. Soc. India*, **34**, 1–24, 1989.

Revenaugh, J. und Jordan, T. H., Mantle layering from ScS reverberations (4 papers), *J. Geophys. Res.*, **103**, 19 749–19 824, 1991.

Rodgers, A. J. und Schwartz, S. Y., Low crustal velocities and mantle lithospheric variations in southern Tibet from regional Pnl waveforms, *Geophys. Res. Lett.*, **24**, 9–12, 1997.

Rodgers, A. J. und Schwartz, S. Y., Lithospheric structure of the Qiangtang Terrane northern Tibetan Plateau, from complete waveform modelling: Evidence for partial melt, *JGR*, **103**, 7137–7152, 1998.

Romanowicz, B. A., Constraints on the structure of the Tibet plateau, *J. Geophys. Res.*, **87**, 6865–6883, 1982.

Rondenay, S., Bostock, M. G., und Shragge, J., Multi-parameter 2-D inversion of scattered teleseismic body-waves–3. Application to the Cascadia 1993 data set, *J. Geophys. Res.*, **106**, 30,795–30,808, 2001.

Roy, S. und Rao, R. U. M., Heat flow in the Indian shield, *J. Geophys. Res.*, **105**, 25,587–25,604, 2000.

Ryberg, T. und Weber, M., Receiver function arrays: A reflection seismic approach, *Geophys. J. Int.*, **141**, 1–11, 2000.

Sandvol, E., Ni, J., Kind, R., und Zhao, W., Seismic anisotropy beneath the southern Himalaya-Tibet collision zone, *J. Geophys. Res.*, **102**, 17,813–17,823, 1997.

Sarkar, D., Kumar, M. R., Saul, J., Kind, R., Raju, P. S., Chadha, R. K., und Shukla, A. K., A receiver function perspective of the Dharwar craton (India) crustal structure, *Geophys. J. Int.*, **in print**, 2003.

Saul, J., Kind, R., und Project INDEPTH Seismic Team, Crustal structure and Poisson's ratio in central Tibet, *suppl. to EOS, Transactions, AGU*, 2000a.

Saul, J., Kumar, M. R., und Sarkar, D., Lithospheric and upper mantle structure of the Indian Shield, from teleseismic receiver functions, *Geophys. Res. Lett.*, **27**, 2357–2360, 2000b.

Savage, M. K., Lower crustal anisotropy or dipping boundaries? Effects on receiver functions and case study in New Zealand, *J. Geophys. Res.*, **103**, 15 069–15 087, 1998.

Shapiro, N. M. und Ritzwoller, M. H., Monte-Carlo inversion for a global shear velocity model of the crust and upper mantle, *Geophys. J. Int.*, **151**, 88–105, 2002.

Shearer, P. M., Seismic imaging of upper mantle structure with new evidence for a 520 km discontinuity, *Nature*, **344**, 121–126, 1990.

Sheehan, A. F., Shearer, P. M., Gilbert, H. J., und Dueker, K. G., Seismic migration processing of P-SV converted phases for mantle discontinuity structure beneath the Snake River Plain, western United States, *J. Geophys. Res.*, **105**, 19.055–19.065, 2000.

Shragge, J., Bostock, M. G., und Rondenay, S., Multi-parameter 2-D inversion of scattered teleseismic body-waves–2. Numerical examples, *J. Geophys. Res.*, **106**, 30,783–30,794, 2001.

Solon, K. D., Jones, A. G., Nelson, K. D., Unsworth, M., und INDEPTH MT Team, Structure of the crust in the vicinity of the Banggong-Nujiang-Suture, central Tibet, from INDEPTH magnetotelluric data, *submitted to J. Geophys. Res.*, 2003.

Tapponnier, P., Zhiqin, X., Roger, F., Meyer, B., Arnaud, N., Wittlinger, G., und Jingsui, Y., Oblique stepwise rise and growth of the Tibet Plateau, *Science*, **294**, 1671–1677, 2001.

Tilmann, F., Ni, J. F., und the INDEPTH Seismic Team, Seismic imaging of the downwelling Indian lithosphere beneath Central Tibet, *Science*, **300**, 1424–1427, 2003.

van der Voo, R., Spakman, W., und Bijwaard, H., Tethyan subducted slabs under india, *Earth and Planetary Science Letters*, **171**, 7–20, 1999.

Vergne, J., Wittlinger, G., Hui, Q., Tapponnier, P., Poupinet, G., Mei, J., Herquel, G., und Paul, A., Seismic evidence for stepwise thickening of the crust across the NE Tibetan Plateau, *Earth and Planetary Science Letters*, **203**, 25–33, 2002.

Vergne, J., Wittlinger, G., Farra, V., und Heping, S., Evidence for upper crustal anisotropy in the Songpan-Ganze terrane, northeastern Tibet, *Geophys. Res. Lett.*, **in print**, 2003.

Vinnik, L. P., Detection of waves converted from P to SV in the mantle, *Phys. Earth and Plan. Int.*, **15**, 39–45, 1977.

Wei, W., Unsworth, M., Jones, A., Booker, J., Tan, H., Nelson, D., Chen, L., Li, S., Solon, K., Bedrosian, P., Jin, S., Deng, M., Ledo, J., Kay, D., und Roberts, B., Detection of widespread fluids in the Tibetan crust by magnetotelluric studies, *Science*, **292**, 716–718, 2001.

Willett, S. D. und Beaumont, C., Subduction of Asian lithospheric mantle beneath Tibet inferred from models of continental collision, *Nature*, **369**, 642–645, 1994.

Yilmaz, O., *Seismic Data Processing*, Society of Exploration Geophysicists, USA, 1987.

Yin, A. und Harrison, T. N., Geologic evolution of the Himalayan-Tibetan orogen, *Annu. Rev. Earth. Planet.*, **28**, 211–280, 2000.

Yuan, X., Ni, J., Kind, R., Mechie, J., und Sandvol, E., Lithospheric and upper mantle structure of southern Tibet from a seismological passive source experiment, *J. Geophys. Res.*, **102**, 27,491–27,500, 1997.

Yuan, X., Sobolev, S., Kind, R., Oncken, O., , Bock, G., Asch, G., Schurr, B., Graeber, F., Rudloff, A., Hanka, W., Wylegalla, K., Tibi, R., Haberland, C., Rietbrock, A., Giese, P., Wigger, P., Röwer, P., Zandt, G., Beck, S., Wallace, T., Pardo, M., und Comte, D., Subduction and collision processes in the Central Andes constrained by converted seismic phases, *Nature*, **408**, 958–961, 2000.

Zandt, G. und Ammon, C. J., Continental crustal composition constrained by measurements of crustal Poisson's ratio, *Nature*, **374**, 152–154, 1995.

Zandt, G., Myers, S. C., und Wallace, T. C., Crust and mantle structure across the Basin and Range-Colorado Plateau boundary at 37°N latitude and implications for cenozoic extensional mechanism, *J. Geophys. Res.*, **100**, 10.529–10.548, 1995.

Zhao, W., Nelson, K. D., und Team, P. I., Deep seismic reflection evidence for continental underthrusting beneath southern Tibet, *Nature*, **366**, 557–559, 1993.

Zhao, W., Mechie, J., Brown, L. D., Guo, J., Haines, S., Hearn, T., Klemperer, S. L., Ma, Y. S., Meissner, R., Nelson, K. D., Ni, J. F., Pananont, P., Rapine, R., Ross, A., und Saul, J., Crustal structure of central Tibet as derived from project INDEPTH seismic data, *Geophys. J. Int.*, **145**, 486–498, 2001.

Zhao, W. L. und Morgan, W. J. P., Injection of Indian crust into Tibetan lower crust: a two-dimensional finite element model study, *Tectonics*, **6**, 489–504, 1987.

Zhu, L. und Kanamori, H., Moho depth variation in southern California from teleseismic receiver functions, *J. Geophys. Res.*, **105**, 2969–2980, 2000.

Zhu, L., Owens, T. J., und Randall, G. E., Lateral variation in crustal structure of the northern Tibetan Plateau inferred from teleseismic receiver functions, *Bull. Seism. Soc. Am.*, **85**, 1531–1540, 1995.

Danksagung

Die vorliegende Arbeit wurde am GeoFoschungsZentrum Potsdam mit finanzieller Unterstützung der Deutschen Forschungsgemeinschaft durchgeführt. Beiden Institutionen gebührt dafür mein herzlicher Dank.

Mein Dank gilt Prof. Dr. Rainer Kind und Dr. Jim Mechie dafür, dass sie mir das Privileg zukommen ließen, ein so interessantes Thema zu bearbeiten und mir weitestgehende Freiheit bei der Ausgestaltung der Arbeit gelassen haben, die sie durch stetige Diskussionsbereitschaft und Anregungen großartig unterstützt haben.

Dr. Günter Asch danke ich für die Übernahme des Zweitgutachtens. Den weiteren Mitgliedern der Prüfungskomission, Prof. Dr. Volker Haak, Oliver Krüger, Prof. Dr. Onno Oncken und Dr. Peter Wigger danke ich, dass sie sich trotz des zu Ende gehenden Semesters die Zeit für eine Beschäftigung mit dieser Arbeit genommen haben.

Meinen Kollegen Mirjam Bohm, Wolfram Geissler, Dr. Winfried Hanka, Benjamin Heit, Barbara Heuer, Karl-Heinz Jäckel, Dr. Jörn Kummerow, Dr. Xuequing Li, Ayman Mohsen, Dr. Bernd Schurr, Forough Sodoudi, Dr. Rigobert Tibi, Ingo Wölbern, Dr. Kurt Wylegalla, Dr. Xiaohui Yuan und ganz besonders Liane Tröger danke ich für das gute Klima in unserer Arbeitsgruppe, ob nun beim Pisco Sour bei “Anita” oder der Tütensuppe im Aufenthaltsraum.

Meinen indischen Kollegen Dr. Ravi Kumar und Dr. Dipankar Sarkar danke ich für die mittlerweile seit acht Jahren bestehende, freundschaftliche Zusammenarbeit und nicht zuletzt für die Bereitstellung eines Teils der in dieser Arbeit verwendeten Daten. Besonderer Dank gilt auch meinen während der Fertigstellung dieser Arbeit verstorbenen Kollegen Dr. Günter Bock und Prof. Doug Nelson.

Ein sehr herzlicher Dank gilt meinen Eltern und meiner Freundin Janeth Gutiérrez, die auf ihre Weise zum Gelingen dieser Arbeit beigetragen haben.

Last but not least danke ich den vielen für mich namenlosen tibetischen Helfern für die oft fast freundschaftliche Zusammenarbeit bei der Feldarbeit, sowie der einheimischen Bevölkerung im Bereich unserer Stationen für den Respekt für unser Projekt und ihre Gastfreundschaft. Der Yakbutter-Tee wird mir ewig in Erinnerung bleiben.

Zusammenfassung

Von Juli 1998 bis Juni 1999 wurde im zentralen Tibet-Plateau die geowissenschaftliche Feldkampagne INDEPTH-3/GEDEPTH-2 durchgeführt, in deren Rahmen 57 seismische Stationen zur Registrierung von Erdbeben für knapp ein Jahr im Feld belassen wurden. Der hierbei gewonnene Datensatz von Registrierungen teleseismischer Beben bildet die Grundlage für eine detaillierte Studie der seismischen Struktur von Kruste und oberem Mantel in Zentral-Tibet.

51 Stationen wurden entlang eines ungefähr linearen Profils von 30,5°N bis 33,8°N installiert, welches sich damit über die nördliche Hälfte des Lhasa- sowie die südliche Hälfte des Qiangtang-Blockes in Zentral-Tibet erstreckte und die Banggong-Nujiang-Sutur etwa in seiner Mitte überquerte.

Zusätzlich zu den Daten des INDEPTH-3/GEDEPTH-2-Experimentes wurden Daten eines neuen Stationsnetzes in Indien analysiert, was einen Vergleich besonders der Struktur des oberen Mantels ermöglicht.

Die Bestimmung der seismischen Struktur erfolgte durch die Isolation von Wellen, welche bei Streuung an stationsseitigen Untergrundstrukturen von P nach S konvertiert wurden (sog. *receiver function*-Methode). Auf der Grundlage von über 4000 *receiver functions* hoher Qualität konnten verschiedene Aspekte der Krustenstruktur im zentralen Tibet-Plateau untersucht werden. Dazu wurde ein Migrationsverfahren entwickelt, welches eine hohe laterale Auflösung ermöglicht. Ein CDP-Stacking-Verfahren wurde weiterentwickelt, um Strukturen auch bei lateral variablen Geschwindigkeiten in ihre korrekte Tiefe projizieren zu können.

Die Krustenmächtigkeit nimmt vom zentralen Lhasa-Block bis in den zentralen Qiangtang-Block nahezu linear von 69 km im Süden auf 62 km im Norden ab. Ein postulierter Sprung in der Moho-Tiefe an der Banggong-Nujiang-Sutur konnte widerlegt werden. Das durchschnittliche krustale Poisson-Verhältnis liegt bei ca. 0,25 im Lhasa- sowie bei 0,28 im Qiangtang-Block, schwankt entlang des INDEPTH-3-Profils aber in einem Bereich von 0,24 bis 0,29. Der P-S-Konversionskoeffizient der Moho variiert stark entlang des Profils. Er ist im Bereich des Qiangtang-Blockes ungefähr doppelt so groß wie im Lhasa-Block, wobei ein Zusammenhang zwischen hohem Poisson-Verhältnis und großem Konversionskoeffizienten zu bestehen scheint. Dieser wird als laterale Variationen der S-Geschwindigkeit besonders in der unteren Kruste interpretiert. Entlang des gesamten Profils werden in ca. 15 bis 30 km Tiefe P-S-Konversionen mit negativem Vorzeichen beobachtet. Diese entsprechen einer Inversion der S-Geschwindigkeiten, welche sich

wahrscheinlich auf partielles Schmelzen oder Fluide in der mittleren Kruste zurückführen lässt. Diese Interpretation wird gestützt durch den Vergleich migrierter *receiver functions* mit Ergebnissen magnetotellurischer Messungen in der Umgebung der Banggong-Nujiang-Sutur, der eine weitestgehende Übereinstimmung der Lage der Geschwindigkeitsinversion mit der Obergrenze einer konduktiven Schicht in der mittleren Kruste ergab. Die Interpretation als partielles Schmelzen bzw. Fluide wird dadurch zusätzlich untermauert.

Unter dem nördlichen Qiangtang-Block konnte der nach Süden subduzierte asiatische lithosphärische Mantel abgebildet werden. Dieser stellt offenbar die untere Begrenzung einer Schicht stark verminderter S-Geschwindigkeiten dar, die nach oben bis fast an die Kruste reicht. Diese Schicht wird als heiße Asthenosphäre interpretiert.

Die Konversionszeiten der Manteldiskontinuitäten in 410 und 660 km Tiefe liegen im indischen Schild nahe denen des globalen IASP91-Modelles, jedoch deutlich über den Zeiten, die in anderen präkambrischen Schilden gemessen werden. Dies wird auf eine anomal dünne indische Lithosphäre zurückgeführt. Der Vergleich mit den entsprechenden Konversionszeiten in Tibet führt nach Anwendung einer Krustenkorrektur auf deutlich kleinere Konversionszeiten, die sich auf eine unter Süd-Tibet verdickte Lithosphäre zurückführen lassen. Die Konversionszeiten entlang des INDEPTH-3/GEDEPTH-2-Profils wiederum sind erheblich größer, mit einem leichten Anstieg nach Norden. Diese Verzögerung wird auf eine Zone reduzierter Geschwindigkeit im oberen Mantel von Zentral-Tibet zurückgeführt, die wahrscheinlich nicht tiefer als 200 km reicht.

Summary

During the period from July 1998 until June 1999 the geophysical/geolocical field experiment INDEPTH-3/GEDEPTH-2 was conducted in the central Tibetan Plateau. As part of the seismological framework, 57 seismic stations where deployed for almost one year to record earthquakes. The recorded data set of teleseismic waveforms form the basis for a detailed study of the seismic structure of crust and upper mantle in central Tibet.

51 stations were installed along an approximately linear profile extending from 30,5°N to 33,8°N, thus covering the northern half of the Lhasa block and the southern half of the Qiangtang block in central Tibet. This profile crossed the Banggong-Nujiang suture near the middle of the line. In addition to the data acquired during INDEPTH-3/GEDEPTH-2, data of permanent seismic networks in India were analyzed, allowing a comparative study of the seismic structure in India and Tibet, with special emphasis on that of the upper mantle.

The seismic structure was determined through isolation of secondary seismic phases, which are converted from P to S through scattering at receiver-side seismic heterogeneities (so-called *receiver function* method). Based on more than 4000 high-quality receiver functions, several aspects of crustal structure in the central Tibetan Plateau were investigated. For that purpose a migration method was developed which allows a high degree of lateral resolution. A CDP stacking tecknique was improved to allow proper depth migration even in the case of laterally varying velocities.

The crustal thickness decreses almost linearly from 69 km in the Lhasa block to 62 km in the central Qiangtang block. A large jump in Moho depth at the Banggong-Nujiang suture postulated by other authors could be rebutted. The average crustal Poisson's ratio averages 0.25 in the Lhasa block and 0.28 in the Qiangtang block, though along the profile it varies within 0.24 - 0.29. The P-S conversion coefficient at the Moho also varies strongly along the profile. Beneath the Qiangtang block the conversion amplitude is about twice as large compared to most of the Lhasa block and there appears to be a relationship between large Poisson's ratio values and Moho conversion amplitudes. This is considered to be an indication of particularly large lateral variations in the structure of the lower crust. Negative-amplitude P-to-S conversions are observed along the whole profile, which correspond to a decrease in S velocity, probably as a consequence of mid-crustal partial melting or fluids. This interpretation is supported by results from a magnetotelluric experiment in the vicinity of the Banggong-Nujiang suture, where the position of the seismic velocity

inversion largely coincides with the upper boundary of a highly conductive mid-crustal layer.

Beneath the northern Qiangtang block, at the northernmost end of the region covered by the INDEPTH-3/GEDEPTH-2 line, the subducting asian lithospheric mantle could be imaged. This structure corresponds to the base of a mantle-wedge-like region of strongly reduced S velocity, which extends almost to the base of the crust and is interpreted as hot asthenospheric material.

The delay times of the waves converted at the mantle discontinuities in 410 and 660 km depth are close to those of the global IASP91 model, but conspicuously delayed compared to the times observed in other Precambrian shield areas. This is interpreted as anomalously thin Indian lithosphere. Comparison with the corresponding delay times in southern Tibet, corrected for the effects of topography and crustal thickness, leads to significantly faster 410 and 660 signals, which can be attributed to a thickened lithosphere beneath southern Tibet. The conversion times along the INDEPTH-3/GEDEPTH-2 profile are in turn slower compared to southern Tibet, with a slight increase towards the northern end of the line. This is consistent with the presence of a low-velocity layer in the upper mantle beneath central Tibet, which appears to be confined to the uppermost 200 km.